CHAPTER-5

INVESTIGATION OF RELATIVISTIC SELF-FOCUSING OF HERMITE-COSINE- GAUSSIAN LASER BEAM IN COLLISIONLESS PLASMA

5.1 INTRODUCTION

The interaction of high power laser beams with plasmas occupies a unique place in the field of research due to wide-ranging applications in laser-driven fusion, laser-driven charged particle accelerators, x-ray lasers etc. [8, 115, 4]. For such applications, it is necessary that the laser beam is highly powerful, intense and propagates for extended distances without divergence, resulting in various nonlinear phenomena like self-focusing etc. Therefore, it is important to study such phenomena numerically and analytically. Since the first investigation on self-trapping of optical beams was reported by Askaryan [1] and later the self-focusing was examined by a number of authors [116, 43, 117]. The self-focusing, self-trapping and filamentation of laser has been theoretically investigated by Akhmanov *et al.* [113] and then developed by Sodha *et al.* [114]. The study of quadruple Gaussian beam in inhomogeneous magnetized plasma with ponderomotive nonlinearity and linear absorption confirms that converging beam shows oscillatory convergence whereas diverging beam shows oscillatory divergence. Further, the beam is more focused at lower intensity under the influence of linear absorption and magnetic field [100]. Kant and Wani [118] reported that the density transition, decentered parameter and linear absorption coefficient act in such a way that they change the self-focusing / defocusing nature of the beam in a significant manner. The absorption weakens the self-focusing effect and density transition sets sooner, early and stronger self-focusing of cosh-Gaussian beam in plasma. The propagation of circularly polarized quadruple Gaussian laser beam can be studied in three different regimes viz steady divergence, oscillatory divergence and self-focusing regime by taking in to account the effect of magnetic field. The magnetic field improves self-focusing for extraordinary mode but, weakens the effect for ordinary mode [101]. An intense laser beam undergoes self-focusing due to the relativistic mass and ponderomotive effects. It then diffracts and focuses more and more during propagation. In order to have sooner and better focusing, the relative plasma density is to be increased. This is because the parameters like density profile and intensity parameter play a vital role for self-focusing [22].

In thermal collisionless quantum plasma, the diffraction effect becomes predominant giving rise to increase in beam width and thus, showing an oscillatory behaviour of beam width parameter. Further, with the increase in plasma density as a ramp slope, the laser beam focuses quickly with lower oscillation amplitude, leads to smaller spot size of laser beam with more oscillations. The laser self-focusing is enhanced more in thermal quantum plasma than in classical regime [97]. However, the magnetic field and plasma density ramp play an important role in the enhancement of self-focusing. This is due to the combined role of magnetic field and density ramp that can reduce the spot size of the beam efficiently close to the axis of propagation [91]. The self-focusing decreases by increasing laser wavelength, ripple wave number and intensity. It is because of the direct dependence of self-focusing on decentered parameter b [94]. Therefore, the phenomenon of self-focusing is obtained by optimizing wavelength and intensity parameters. Moreover, the decentered parameter and ramp density profile are sensitive to the self-focusing of laser beam. It is the density ramp that shrinks the spot size of laser beam as it gets penetrated deeper in to the plasma. Due to which the laser becomes more focussed and can propagate over a long distance without divergence [92]. Further, the proper selection of decentered parameter is important for stronger self-focusing [90]. Gill *et al.* [81] used the condition for the formation of a dark and bright ring to study the focusing / defocusing of super-Gaussian laser beam in plasma with transverse magnetic field. They included higher order terms of the dielectric function and reported that the inclusion of such terms affects the beam width parameter variation and consequently substantial increase in self-focusing is observed. This is possible only in case of the dark ring. However, the results contradict in case of a bright ring. Under the ponderomotive self-focusing, the pulse acquires a minimum spot size due to the role of plasma density ramp. It then diffracts and gets focused in a periodic manner because of the fact that channel size and spot size do not match together. In such a case the oscillation amplitude of the spot size decreases, while its frequency increases. Further, as the plasma density increases under plasma density ramp, the beam gets more focused. However, in the absence density ramp and due to supremacy of the diffraction effect, it gets defocused [77]. The quantum effect gives more self-focusing in comparison to that of classical relativistic case. This is due to the fact that the beam is weaker at high intensity for classical relativistic case than cold quantum case [84].

The initial beam profile of HcosG beam remains invariant during propagation. However, in uniaxial crystals, the initial symmetry and linear polarization of HcosG beam cannot be kept intact. In addition the distribution of field of HcosG beam is closely related to the decentered parameter. In this paper, the relativistic self-focusing of HcosG beam in collisionless plasma is investigated. Using WKB and paraxial approximations through the parabolic equation, a mathematical formulation for the beam width parameter in collisionless plasma is obtained from the wave equation. The evolution of beam width parameter with the propagation distance is presented. It is hereby noticed that the laser self-focusing increases more than predicted by Aggarwal *et al.* [101]. Moreover, the effect of parameters like decentered parameter, laser intensity and initial plasma density is investigated. We previously studied the self-focusing of HchG beam in plasma under density transition [119] and found that self-focusing occurs under the influence of density ramp and decentered parameter. However, in the present communication, the authors lay emphasis on relativistic self-focusing of HcosG laser beam propagating in underdense plasma which was not done earlier for such a beam as per the literature available at present. The importance of the present work lies in the fact that an increase in self-focusing length leads to decrease in the minimum spot size of the beam and hence modulates the phenomenon of self-focusing. The computational results in context of plasma density, decentered parameter and laser intensity are discussed and finally a brief conclusion is given in the last section of this chapter. Above all in the present analysis the decentered parameter and laser intensity has good impact on the propagation of HcosG beam in plasma.

5.2 FIELD DISTRIBUTION OF HERMITE – COSINE – GAUSSIAN (HCOSG) BEAM

Consider the HcosG laser beam propagating in collisionless plasma along z-axis having field distribution of the form

$$E(x,y,z)=\frac{E_0}{\sqrt{f_1(z)f_2(z)}}H_m\left(\frac{\sqrt{2}x}{r_0 f_1(z)}\right)H_n\left(\frac{\sqrt{2}y}{r_0 f_2(z)}\right)\exp\left[-\left(\frac{x^2}{r_0^2 f_1^2(z)}+\frac{y^2}{r_0^2 f_2^2(z)}\right)\right]\times$$

$$\cos\left(\frac{\Omega_0 x}{f_1(z)}\right)\cos\left(\frac{\Omega_0 y}{f_2(z)}\right) \tag{5.1}$$

where H_m and H_n are the m^{th} and n^{th} order Hermite polynomial respectively, E_0 is the constant

amplitude of the electric field, r_0 is the waist width, Ω_0 is the parameter associated with the cosine function, $f_1(z)$ and $f_2(z)$ are the beam width parameters in x and y directions respectively.

5.3 NONLINEAR DIELECTRIC CONSTANT

Consider the propagation of HcosG laser beam in plasma characterized by dielectric constant of the fo

$$\varepsilon = \varepsilon_0 + \phi(EE^*) \tag{5.2}$$

with $\varepsilon_0 = 1 - \omega_p^2 / \omega^2$, $\omega_p^2 = 4\pi n_0 e^2 / m$, $m = m_0\gamma$. Where, $\gamma = 1/\sqrt{1 - v^2/c^2}$, m_0 and e are the rest mass and charge on the electron. Therefore, $\omega_p^2 = \omega_{p0}^2 / \gamma$, $\omega_{p0}^2 = 4\pi n_0 e^2 / m_0$, ϕ represents the nonlinear part of the dielectric constant, ω is the angular frequency of laser beam, ω_p is plasma frequency, n_0 is the equilibrium electron density, R_d is the diffraction length and ξ is the normalized propagation distance.

The nonlinear dielectric constant for collisionless plasma can be expressed as [114]

$$\phi(EE^*) = \frac{\omega_{p0}^2}{\gamma\omega^2}\left[1 - \exp\left(-\frac{3m_0\gamma}{4M}\alpha EE^*\right)\right] \tag{5.3}$$

Where $\alpha = e^2 M / 6m_0^2\gamma^2\omega^2 k_B T$ and M is the mass of scaterrer, T is the plasma temperature and k_B is the Boltzmann constant.

5.4 SELF-FOCUSING EQUATIONS

The wave equation describing the laser beam propagation may be written as

$$\nabla^2\vec{E} - \frac{\varepsilon}{c^2}\left(-\omega^2\vec{E}\right) + \vec{\nabla}\left(\frac{\vec{E}\vec{\nabla}\cdot\varepsilon}{\varepsilon}\right) = 0 \tag{5.4}$$

The last term of equation (5.4) on left hand side is neglected under the condition that $k^{-2}\nabla^2(\ln\varepsilon) << 1$, where 'k'represents the wave number the laser beam. Thus,

$$\nabla^2\vec{E} + \frac{\omega^2}{c^2}\varepsilon\vec{E} = 0 \tag{5.5}$$

In Cartesian co-ordinate system, we can write this equation as

$$\frac{\partial^2 \vec{E}}{\partial x^2} + \frac{\partial^2 \vec{E}}{\partial y^2} + \frac{\partial^2 \vec{E}}{\partial z^2} + \varepsilon \frac{\omega^2}{c^2} \vec{E} = 0 \qquad (5.6)$$

The solution of equation (5.6) is of the following form,

$$\vec{E} = A(x, y, z) Exp[i(\omega t - kz)] \qquad (5.7)$$

With $k^2 = \varepsilon_0 \, \omega^2 / c^2$.

Differentiating equation (3.11) twice w. r. t. 'x, y and z respectively , we get

$$\frac{\partial \vec{E}}{\partial x} = Exp[i(\omega t - kz)] \frac{\partial A}{\partial x}$$

$$\frac{\partial^2 \vec{E}}{\partial x^2} = Exp[i(\omega t - kz)] \frac{\partial^2 A}{\partial x^2}$$

$$\frac{\partial \vec{E}}{\partial y} = Exp[i(\omega t - kz)] \frac{\partial A}{\partial y}$$

$$\frac{\partial^2 \vec{E}}{\partial y^2} = Exp[i(\omega t - kz)] \frac{\partial^2 A}{\partial y^2}$$

Similarly,

$$\frac{\partial^2 \vec{E}}{\partial z^2} = Exp[i(\omega t - kz)] \left[\frac{\partial^2 A}{\partial z^2} - 2ik \frac{\partial A}{\partial z} - k^2 A \right]$$

Neglecting, $\frac{\partial^2 A}{\partial z^2}$, we get

$$\frac{\partial^2 \vec{E}}{\partial z^2} = -Exp[i(\omega t - kz)] \left[2ik \frac{\partial A}{\partial z} + k^2 A \right]$$

Therefore, using the above values, Eq. (5.6), under Wentzel-Kramers-Brillouin (WKB) approximation becomes as:

$$2ik \frac{\partial A}{\partial z} = \frac{\partial^2 A}{\partial x^2} + \frac{\partial^2 A}{\partial y^2} + \frac{k^2}{\varepsilon_0} \Phi(AA^*) A = 0 \qquad (5.8)$$

To solve equation (5.8) we express A as

$$A(x, y, z) = A_{mn}(x, y, z) \exp[-ikS(x, y, z)] \qquad (5.9)$$

Where, $k = (\omega / c)\varepsilon_0^{1/2}$ and A_{mn} and S depend on x, y and z. Differentiating Eq. (5.9) w. r. t. 'x, y and z , we get

$$\frac{\partial \vec{A}}{\partial x} = Exp\left[-iKS(x,y,z)\right]\left[\frac{\partial A_{mn}}{\partial x} - ikA_{mn}\frac{\partial S}{\partial x}\right]$$

$$\frac{\partial^2 \vec{A}}{\partial x^2} = Exp\left[-iKS(x,y,z)\right]\left[\frac{\partial A^2{}_{mn}}{\partial x^2} - ikA_{mn}\frac{\partial^2 S}{\partial x^2} - 2ik\frac{\partial S}{\partial x}\frac{\partial A_{mn}}{\partial x} - k^2 A_{mn}\left(\frac{\partial S}{\partial x}\right)^2\right]$$

Similarly,

$$\frac{\partial^2 \vec{A}}{\partial y^2} = Exp\left[-iKS(x,y,z)\right]\left[\frac{\partial A^2{}_{mn}}{\partial y^2} - ikA_{mn}\frac{\partial^2 S}{\partial y^2} - 2ik\frac{\partial S}{\partial y}\frac{\partial A_{mn}}{\partial y} - k^2 A_{mn}\left(\frac{\partial S}{\partial y}\right)^2\right]$$

$$\frac{\partial \vec{A}}{\partial z} = Exp\left[-iKS(x,y,z)\right]\left[\frac{\partial A_{mn}}{\partial z} - ikA_{mn}\frac{\partial S}{\partial z}\right]$$

Substituting the above values in Eq. (5.8), we get

$$2ik\left[\frac{\partial A_{mn}}{\partial z} - ikA_{mn}\frac{\partial S}{\partial z}\right] = \frac{\partial A^2{}_{mn}}{\partial x^2} + \frac{\partial A^2{}_{mn}}{\partial y^2} - ikA_{mn}\left(\frac{\partial^2 S}{\partial x^2} + \frac{\partial^2 S}{\partial y^2}\right) - 2ik\left(\frac{\partial S}{\partial x}\frac{\partial A_{mn}}{\partial x} + \frac{\partial S}{\partial y}\frac{\partial A_{mn}}{\partial y}\right)$$
$$- k^2 A_{mn}\left[\left(\frac{\partial S}{\partial x}\right)^2 + \left(\frac{\partial S}{\partial y}\right)^2\right] + \frac{k^2\phi(A_{mn}^2)A_{mn}}{\varepsilon_0} \qquad (5.10)$$

Now, equating real and imaginary parts on both sides of Eq. (5.10), we get

Real part equation is

$$2\left(\frac{\partial S}{\partial z}\right) + \left(\frac{\partial S}{\partial x}\right)^2 + \left(\frac{\partial S}{\partial y}\right)^2 = \frac{1}{k^2 A_{mn}}\left(\frac{\partial^2 A_{mn}}{\partial x^2} + \frac{\partial^2 A_{mn}}{\partial y^2}\right) + \frac{\phi(A_{mn}^2)}{\varepsilon_0} \qquad (5.11)$$

Imaginary part equation is

$$\frac{\partial A_{mn}^2}{\partial z} + \frac{\partial S}{\partial x}\frac{\partial A_{mn}^2}{\partial x} + \frac{\partial S}{\partial y}\frac{\partial A_{mn}^2}{\partial y} + A_{mn}^2\left(\frac{\partial^2 S}{\partial x^2} + \frac{\partial^2 S}{\partial y^2}\right) = 0 \qquad (5.12)$$

The solutions of equations (5.11) and (5.12) can be written as:

$$A_{mn}^2 = \frac{E_0^2}{f_1(z) f_2(z)} H_m\left(\frac{\sqrt{2}x}{r_0 f_1(z)}\right) H_n\left(\frac{\sqrt{2}y}{r_0 f_2(z)}\right) \exp\left[-\left(\frac{x^2}{r_0^2 f_1^2(Z)} + \frac{y^2}{r_0^2 f_2^2(z)}\right)\right] \times$$

$$\cos\left(\frac{\Omega_0 x}{f_1(z)}\right) \cos\left(\frac{\Omega_0 y}{f_2(z)}\right) \tag{5.13}$$

And

$$S = \frac{x^2}{2}\beta_1(z) + \frac{y^2}{2}\beta_2(z) + \varphi(z) \tag{5.14}$$

Where, $\beta_1(z) = (1/f_1(z))(\partial f_1/\partial z)$ and $\beta_2(z) = (1/f_2(z))(\partial f_2/\partial z)$ represent the curvature of the wavefront in x and y directions respectively. Now, considering the mode for which, m = 0 and n = 0, we have, $H_0\left(\sqrt{2}x/(r_0 f_1(z))\right)=1$ and $H_0\left(\sqrt{2}y/(r_0 f_2(z))\right)=1$. Further, employing the paraxial approximation and differentiating Eq. (5.13) and (5.14), we get

$$\frac{\partial A_{mn}}{\partial x} = \frac{-E_0}{\sqrt{f_1 f_2}} \sqrt{\cos\left(\frac{\Omega_0 y}{f_2}\right)} Exp\left[-\frac{1}{2r_0^2}\left(\frac{x^2}{f_1^2} + \frac{y^2}{f_2^2}\right)\right] \left(\frac{\Omega_0}{2f_1} \frac{\sin\left(\frac{\Omega_0 x}{f_1}\right)}{\sqrt{\cos\left(\frac{\Omega_0 x}{f_1}\right)}} + \frac{x\sqrt{\cos\left(\frac{\Omega_0 x}{f_1}\right)}}{r_0^2 f_1^2}\right)$$

$$\frac{\partial^2 A_{mn}}{\partial x^2} = A_{mn}\left[\frac{\Omega_0 x}{r_0^2 f_1^3}\tan\left(\frac{\Omega_0 x}{f_1}\right) - \frac{\Omega_0^2}{4f_1^2}\tan^2\left(\frac{\Omega_0 x}{f_1}\right) + \frac{x^2}{r_0^4 f_1^4} - \frac{\Omega_0^2}{2f_1^2} - \frac{1}{r_0^2 f_1^2}\right]$$

Similarly, $\frac{\partial^2 A_{mn}}{\partial y^2} = A_{mn}\left[\frac{\Omega_0 y}{r_0^2 f_2^3}\tan\left(\frac{\Omega_0 y}{f_2}\right) - \frac{\Omega_0^2}{4f_2^2}\tan^2\left(\frac{\Omega_0 y}{f_2}\right) + \frac{y^2}{r_0^4 f_2^4} - \frac{\Omega_0^2}{2f_2^2} - \frac{1}{r_0^2 f_2^2}\right]$

And $\frac{\partial S}{\partial x} = x\beta_1, \frac{\partial S}{\partial y} = x\beta_2 and \frac{\partial S}{\partial z} = \frac{x^2}{2}\frac{\partial \beta_1}{\partial z} + \frac{y^2}{2}\frac{\partial \beta_2}{\partial z} + \frac{\partial \varphi}{\partial z}$

Therefore, using the above values in Eq. (5.11), we get

$$x^2\left(\frac{1}{f_1}\frac{\partial^2 f_1}{\partial z^2}\right) + y^2\left(\frac{1}{f_2}\frac{\partial^2 f_2}{\partial z^2}\right) + 2\frac{\partial \varphi}{\partial z} = \frac{1}{k^2}\left[\frac{\Omega_0 x}{r_0^2 f_1^3}\tan\left(\frac{\Omega_0 x}{f_1}\right) - \frac{\Omega_0^2}{4f_1^2}\tan^2\left(\frac{\Omega_0 x}{f_1}\right) + \frac{x^2}{r_0^4 f_1^4}\right]$$

$$= \frac{1}{k^2}\left[-\frac{\Omega_0^2}{2f_1^2} - \frac{1}{r_0^2 f_1^2} + \frac{\Omega_0 y}{r_0^2 f_2^3}\tan\left(\frac{\Omega_0 y}{f_2}\right) - \frac{\Omega_0^2}{4f_2^2}\tan^2\left(\frac{\Omega_0 y}{f_2}\right) + \frac{y^2}{r_0^4 f_2^4} - \frac{\Omega_0^2}{2f_2^2} - \frac{1}{r_0^2 f_2^2}\right]$$
$$- \frac{E_0^2 \Phi'(A_{mn}^2)}{\varepsilon_0 r_0^2 f_1 f_2}\left(1 + \frac{r_0^2\Omega_0^2}{2}\right)\left(\frac{x^2}{f_1^2} + \frac{y^2}{f_2^2}\right) \qquad (5.15)$$

Now, equating the coefficients of x^2 and y^2 on both sides of Eq. (5.15) and using $\xi = z/R_d$, where, $R_d = kr_0^2$ we get

$$\frac{\partial^2 f_1}{\partial \xi^2} = \frac{1}{f_1^3} - \frac{E_0^2 R_d^2 \Phi'(A_{mn}^2)}{\varepsilon_0 r_0^2 f_1^2 f_2}\left(1 + \frac{r_0^2\Omega_0^2}{2}\right) \qquad (5.16)$$

Similarly,

$$\frac{\partial^2 f_2}{\partial \xi^2} = \frac{1}{f_2^3} - \frac{E_0^2 R_d^2 \Phi'(A_{mn}^2)}{\varepsilon_0 r_0^2 f_2^2 f_1}\left(1 + \frac{r_0^2\Omega_0^2}{2}\right) \qquad (5.17)$$

Where, $\Phi'(A_{mn}^2) = \left(\frac{\omega_{p0}}{\omega}\right)^2\left(\frac{3m_0\alpha}{4M}\right)\exp\left[-\left(\frac{3}{4}\right)\left(\frac{m_0\gamma}{M}\right)\left(\frac{\alpha E_0^2}{f_1 f_2}\right)\right]$

After simplifying the equations (5.16) and (5.17), we obtain the expressions for beam width parameters f_1 and f_2 as:

$$\frac{\partial^2 f_1(z)}{\partial \xi^2} = \frac{1}{f_1^3} - \left(\frac{3}{4}\right)\left(\frac{m_0}{M}\right)\left(\alpha E_0^2\right)\left(\frac{\omega_{p0}}{\omega}\right)^2\left(\frac{r_0\omega}{c}\right)^2\frac{(1+b^2/2)}{f_1^2 f_2}\exp\left[-\left(\frac{3}{4}\right)\left(\frac{m_0\gamma}{M}\right)\left(\frac{\alpha E_0^2}{f_1 f_2}\right)\right] \qquad (5.18)$$

And

$$\frac{\partial^2 f_2(z)}{\partial \xi^2} = \frac{1}{f_2^3} - \left(\frac{3}{4}\right)\left(\frac{m_0}{M}\right)\left(\alpha E_0^2\right)\left(\frac{\omega_{p0}}{\omega}\right)^2\left(\frac{r_0\omega}{c}\right)^2\frac{(1+b^2/2)}{f_2^2 f_1}\exp\left[-\left(\frac{3}{4}\right)\left(\frac{m_0\gamma}{M}\right)\left(\frac{\alpha E_0^2}{f_1 f_2}\right)\right] \qquad (5.19)$$

where $b = r_0\Omega_0$ is called decentered parameter and ξ is the dimensionless distance of propagation. Equations (5.18) and (5.19) are the required expressions for beam width parameters f_1 and f_2 respectively.

5.5 SELF-TRAPPED CONDITION

For initially plane wavefront, $(\partial f_1/\partial\xi)_{\xi=0}=0$, $(f_1)_{\xi=0}=1$ and $(\partial f_2/\partial\xi)_{\xi=0}=0$, $(f_2)_{\xi=0}=1$, the conditions $\partial^2 f_1/\partial\xi^2=0$ and $\partial^2 f_2/\partial\xi^2=0$ lead to the propagation of laser beam in self-trapped mode. Substituting for $\partial^2 f_1/\partial\xi^2=0$ and $\partial^2 f_2/\partial\xi^2=0$ in Eq. (5.18) and Eq. (5.19) respectively, we obtain a relation for dimensionless initial beam width $\rho_0 (=r_0\omega/c)$ and is given as follows:

$$\rho_0=\left\{\frac{\exp\left[\left(\frac{3}{4}\right)\left(\frac{m_0\gamma}{M}\right)\left(\alpha E_0^2\right)\right]}{\left(\frac{3}{4}\right)\left(\frac{m_0}{M}\right)\left(\alpha E_0^2\right)(1+b^2/2)}\right\}^{1/2} \tag{5.20}$$

To explain the results for HcosG beam propagation in relativistic plasma, we numerically analyze the dependence of initial beam width ρ_0 as a function of αE_0^2 for the plasma under self-trapped condition. The results are depicted in Fig. 5.1. It is found that decrease in ρ_0 is observed with increase in αE_0^2 for relativistic plasma at different values of decentered parameter.

5.6 RESULTS AND DISCUSSION

We conduct the numerical analysis and computational simulations for solving the beam width parameter equations. The various parameters chosen for the purpose of numerical calculations are: $\omega=10^{14}\,rad/\sec$, $\omega_{p0}=1.87\times10^{14}\,rad/\sec$, $r_0=5\times10^{-3}\,cm$ and $n_0=9.98\times10^{17}\,cm^{-3}$ [71].

The relativistic nonlinear effect emerging from the relativistic mass correction that depends on factor αE_0^2 and relative plasma density ω_{p0}/ω. The diffractional divergence of the beam is due to the diffraction term while as self-focusing is due to nonlinear term. Fig. 5.2 shows the dependence f on ξ for various values of $b=0,0.5\,\&\,1$ with $\omega_{p0}/\omega=0.4$ and $\alpha E_0^2=1.5$. It is clear from fig. 5.2 that strong self-focusing occurs at $\xi=2.65$ for $b=1$ and at $\xi=3.1$ for $b=0.5$. Decentered parameter is an important parameter that is to be optimized for stronger self-focusing at smaller distance. This is because of the fact that the decentered parameter changes the nature of

self-focusing of the beam significantly. Fig.5.3, illustrates the behaviour of f with ξ for $\alpha E_0^2 = 1,1.25 \& 1.50$. It is obvious from the figure that sharp self-focusing is observed at $\xi = 3.1$. It is seen from fig. 5.3 that as we increase the values of αE_0^2, self-focusing occurs earlier and becomes stronger. This is because of the supremacy of self-focusing term over the diffraction term because of the relativistic nonlinearity.

Fig. 5.4 shows the dependence f on ξ for various values $b = 0,1 \& 2$ with $\omega_{p0} / \omega = 0.6$ and $\alpha E_0^2 = 2$. It has been predicted that by increasing the values b, f decreases greatly up to $\xi = 2.35$, there by showing that the self-focusing of laser beam is enhanced further. Further, it can be seen that for a high intensity laser, the self-focusing occurs at lower values of b. Therefore, the decentered parameter is sensitive for the self-focusing of HcosG laser beam and thus, supports the results predicted by Nanda *et al.* [90]. Moreover, the beam converges more rapidly and focuses up to smaller spot size. The beam width parameter decreases monotonically with intensity, decentered parameter and plasma density. Finally, to through light up on the nature of self-focusing of HcosG laser beam in collisionless plasma, in Fig. 5.5, we observe the stronger and earlier self-focusing (corresponding to $\xi = 0.25$) of laser beam as a result of increase in plasma density. This is due to the fact that when the plasma density is increased at relativistic intensities, the beam having more relativistic electrons travels with the laser pulse. With the result, a higher current and consequently a high magnetic field is generated, which leads to further enhancement of self-focusing.

5.7 CONCLUSION

We have investigated the self-focusing of HcosG laser beam in collisionless plasma by taking in to account the relativistic nonlinearity, using WKB and paraxial approximation. The equation of beam width parameter and self-trapped mode has been derived under the weak relativistic ponderomotive nonlinearity. Depending on the values of decentered parameter, laser intensity and plasma density, the variation of dimensionless beam width parameter as a function of normalized propagation distance is seen and discussed. We have found that the laser beam focuses faster and earlier with smaller spot size. The spot size can be controlled by optimizing laser plasma parameters. Thus, one may conclude that the decentered parameter and laser

intensity has a significant role in improving self-focusing of HcosG laser beam in plasma. It is expected that the results of present analysis may be useful in laser driven fusion.

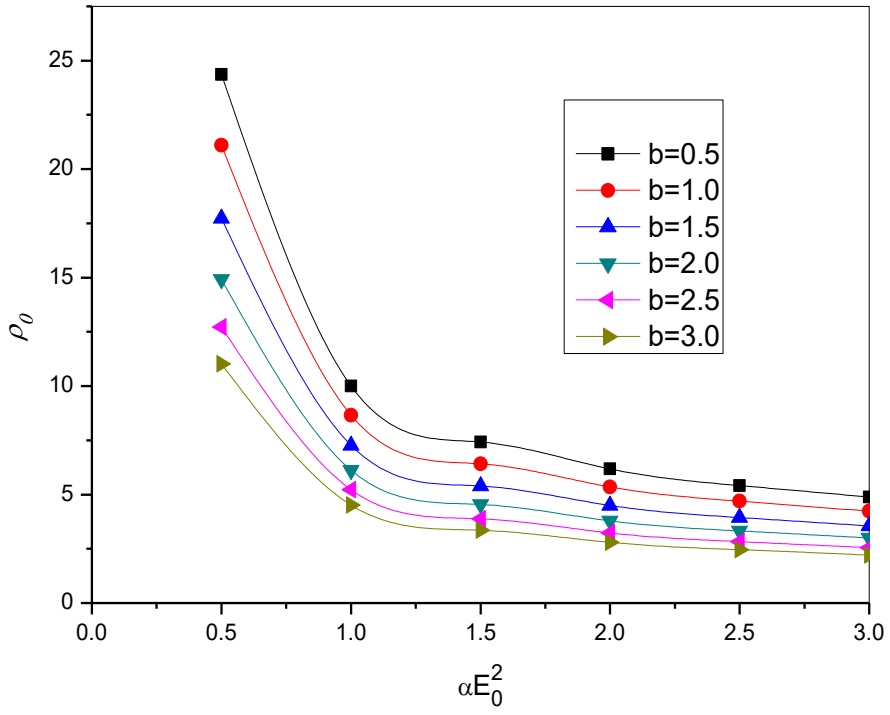

Figure 5.1: Dependence of $\rho_0(r_0\omega_{p0}/c)$ on αE_0^2 for m_0/M = 0.02 and γ = 1.25

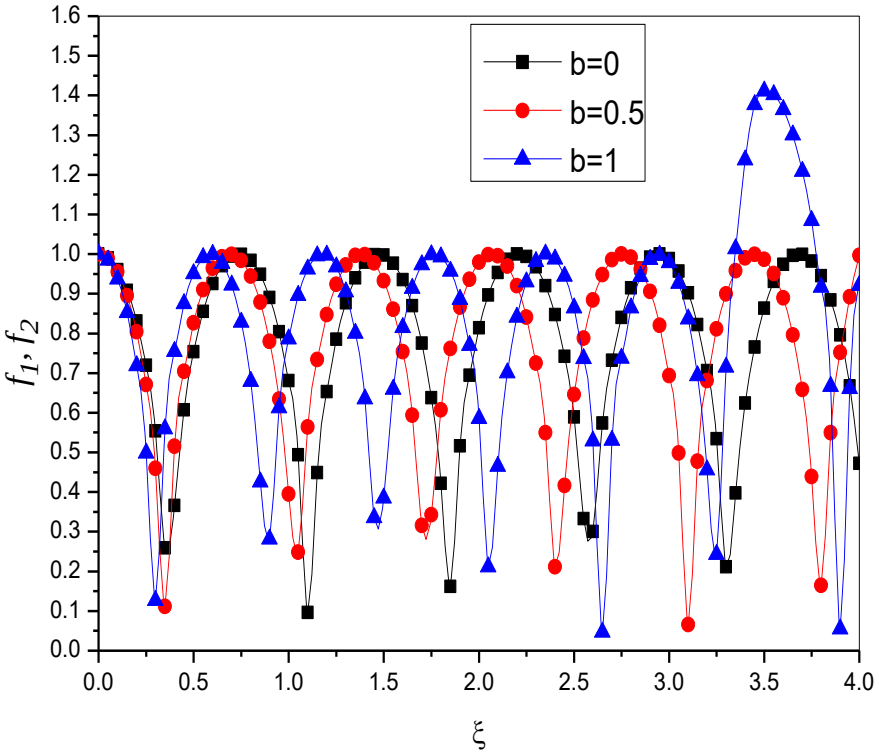

Figure 5.2: Dependence of f_1 and f_2 on ξ for various values of b. The other parameters are $\omega_{p0}/\omega = 0.6,\ \alpha E_0^2 = 1.5,\ m_0/M = 0.02,\ r_0\omega/c = 50,\ \gamma = 1.25$

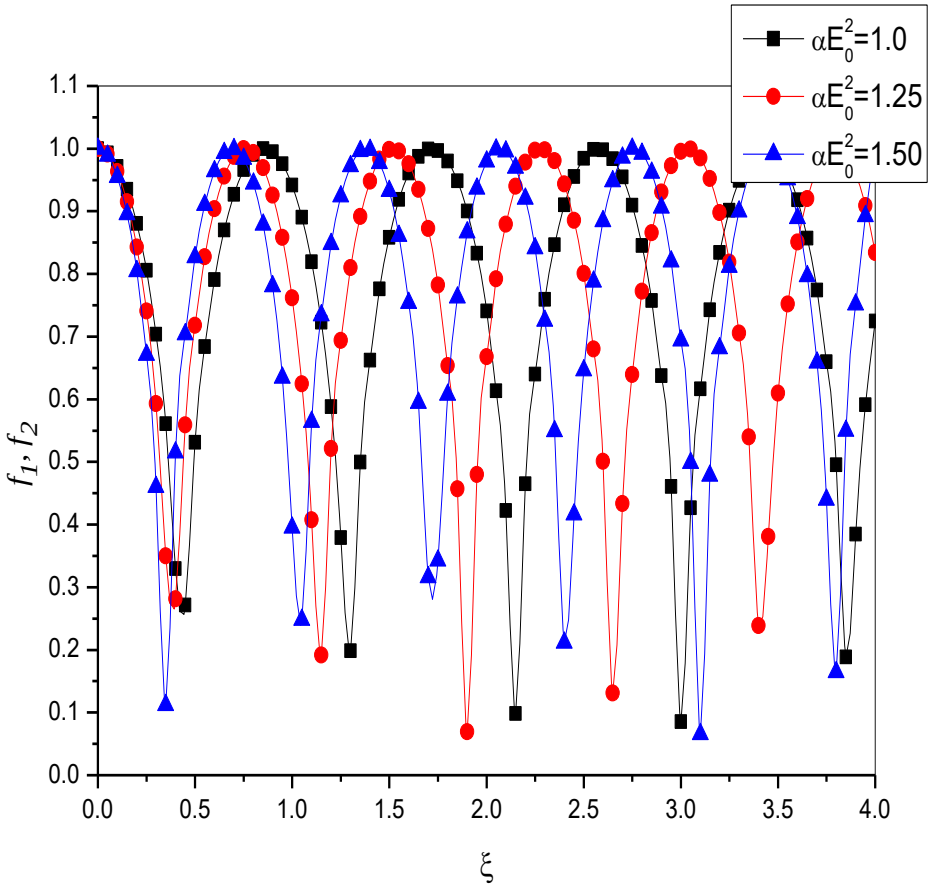

Figure 5.3: Dependence of f_1 and f_2 on ξ for various values of αE_0^2. The other parameters are $\omega_{p0}/\omega = 0.4,\ b = 0.5,\ m_0/M = 0.02,\ r_0\omega/c = 50,\ \gamma = 1.25$

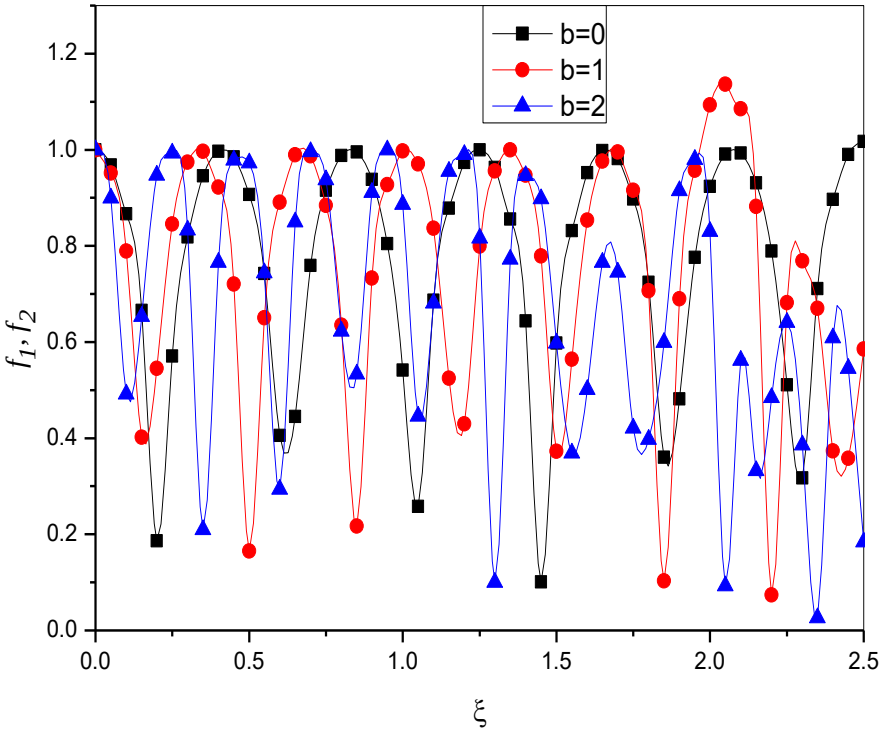

Figure 5.4: Dependence of f_1 and f_2 on ξ for various values of b. The other parameters are $\omega_{p0}/\omega = 0.6,\ \alpha E_0^2 = 2,\ m_0/M = 0.02,\ r_0\omega/c = 50,\ \gamma = 1.40$

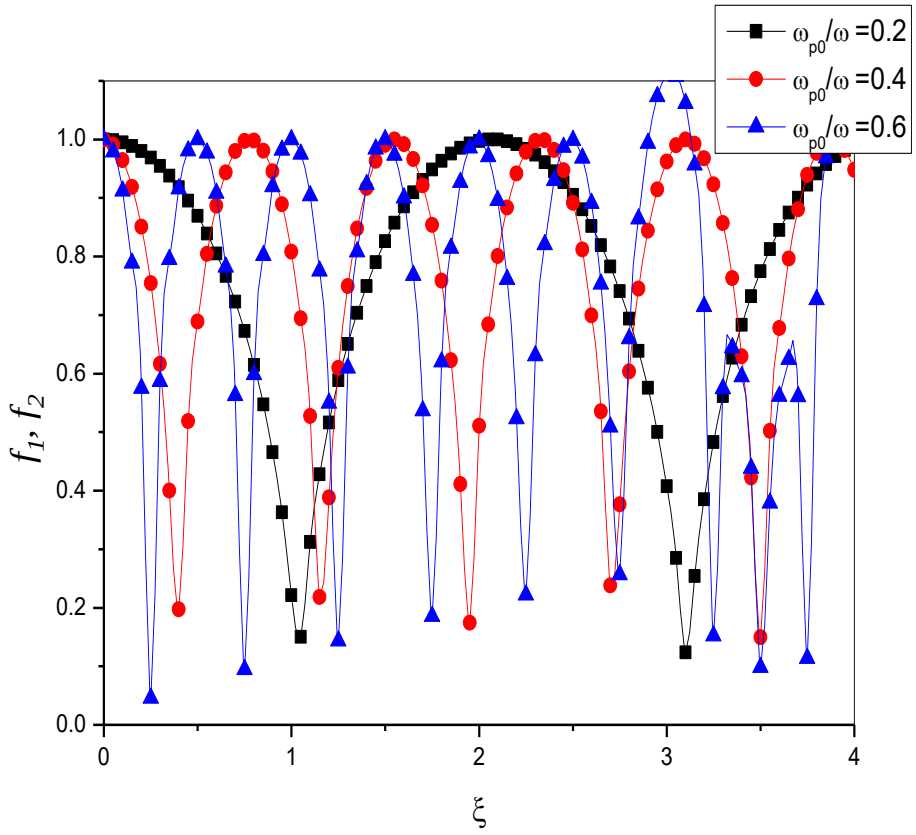

Figure 5.5: Dependence f_1 and f_2 on ξ for various values of ω_{p0}/ω. The other parameters are $\alpha E_0^2 = 1.2,\ m_0/M = 0.02,\ r_0\omega/c = 50,\ \gamma = 1.25$ and $b = 0.5$